Infection dynamics of a V. splendidus strain pathogenic to Mytilus edulis: In vivo and in vitro interactions with hemocytes

Yosra Ben Cheikh, Marie-Agnès Travers, Frank Le Foll

▶ **To cite this version:**

Yosra Ben Cheikh, Marie-Agnès Travers, Frank Le Foll. Infection dynamics of a V. splendidus strain pathogenic to Mytilus edulis: In vivo and in vitro interactions with hemocytes. Fish and Shellfish Immunology, 2017, 70, pp.515-523. 10.1016/j.fsi.2017.09.047 . hal-01738542

HAL Id: hal-01738542

https://normandie-univ.hal.science/hal-01738542

Submitted on 20 Mar 2018

HAL is a multi-disciplinary open access archive for the deposit and dissemination of scientific research documents, whether they are published or not. The documents may come from teaching and research institutions in France or abroad, or from public or private research centers.

L'archive ouverte pluridisciplinaire **HAL**, est destinée au dépôt et à la diffusion de documents scientifiques de niveau recherche, publiés ou non, émanant des établissements d'enseignement et de recherche français ou étrangers, des laboratoires publics ou privés.

Infection dynamics of a *V. splendidus* strain pathogenic to *Mytilus edulis*: *in vivo* and *in vitro* interactions with hemocytes

Yosra Ben Cheikh[a], Marie-Agnès Travers[b] and Frank Le Foll[a]

Authors affiliation

[a] UMR-I 02 INERIS-URCA-ULH SEBIO / Environmental stresses and aquatic biomonitoring, FR CNRS 3730 Scale, Université Le Havre Normandie, F-76063, Le Havre Cedex, France

[b] Ifremer, SG2M-LGPMM, Laboratoire de Génétique et Pathologie des Mollusques Marins Avenue de Mus de Loup, 17390 La Tremblade, France.

Corresponding Author

Yosra Ben Cheikh
E-mail: yosra_bencheikh@yahoo.fr
Tel +33 (0)2 32 74 43 79

Abstract

The pathogenic strain *V. splendidus* 10/068 1T1 has previously been reported for its virulence to the blue mussel and for its capacity to alter immune responses. In this study, we expanded the knowledge on hemocyte-pathogen interactions by using *in vitro* and *in vivo* assays. *V. splendidus* 10/068 1T1 severely inhibited cell adhesion and acidic vacuole formation unlike the innocuous phylogenetically related *V. splendidus* 12/056 M24T1 which had no effect on these cell functions. Furthermore, the virulent bacteria decreased hemocyte viability (59% of viability after 24h). Infection dynamics were explored by using a model based on water tank cohabitation with septic mussels infected by GFP-tagged *V. splendidus* 10/068 1T1. Experimental infections were successfully produced (16.6% and 45% mortalities in 3 days and 6 days). The amount of GFP *Vibrio* in seawater decreased during the experiment suggesting its horizontal transfer from diseased animals to healthy ones. At the same time periods, bacteria were detected in hemocytes and in various organs and caused necrosis especially in gills. Total hemocyte count and viability were affected. Taken together, our results indicate that the pathogen *V. splendidus* 10/068 1T1 colonizes its host both by bypassing external defense barriers and impairing hemocyte defense activities.

Keywords: innate immunity, bivalves, *Vibrio*, infection, experimental model, hemocyte

1. Introduction

Heterotrophic bacteria belonging to the genus *Vibrio* are highly abundant in the aquatic environment, mostly in seawater [1]. These ubiquitous microorganisms persist in a variety of geographic areas in interaction with eukaryotic marine hosts including zooplankton, sponges, corals and molluscs [1]. *Vibrio* sp. show a remarkable biodiversity. Until now, more than 110 species of *Vibrios* have been identified, displaying a variety of host association modalities that extend from symbiosis to virulent pathogenicity [2,3].

Many species of pathogenic *Vibrios* are known to be responsible for diseases in terrestrial or marine vertebrates and invertebrates. *Vibrio cholerae, Vibrio vulnificus* and *Vibrio parahaemolyticus* in particular cause severe disorders in humans [4,5]. In numerous aquatic organisms including fish [6], corals [7], shrimp [8] and shellfish [9], some *Vibrio*s have been associated with serious infections. Because of the high economic loss generated in the aquaculture sector, many studies are dedicated to bacterial diseases, particularly in farmed bivalves [3,9,10]. Among the etiological agents, bacteria from the clade *Splendidus* have been repeatedly described in relation to mortality events. This polyphyletic group include 16 species with contrasted pathotypes [11,12]. Different strains have been implicated in mortalities of various bivalves, e.g. the Pacific oyster *Crassostrea gigas* [13–17], the Atlantic scallop *Pecten maximus* [18,19], the carpet shell clam *Ruditapes philippinarum* [20], the greenshell mussel *Perna canaliculus* [21] and recently the blue mussel *Mytilus edulis* [11].

While infection mechanisms are well studied in human invaders, little is known in the specific case of invertebrate pathogens. Some results have been gathered in different species, especially concerning host-pathogen interactions [11, 22–24]. However, invasion processes remain poorly documented. Understanding infection dynamics is an essential step for developing diseases management strategies [25]. In particular, there is a need for robust and standardized experimental models of *Vibrio*-bivalve interactions.

In a previous work, from mortality events reported by mussel farmers, we have isolated a *Vibrio* strain virulent to the blue mussel. *V. splendidus* 10/068 1T1 has been shown to alter hemocyte phagocytosis capacities, a key parameter of the immune defense system in mussels. Furthermore, a stable GFP-tagged *Vibrio* strain was constructed to facilitate the study of interactions between the microorganism and immune cells [11]. Fluorescent proteins (FP)-tagged microorganisms constitute a useful tool to monitor colonization processes. They have been used to elucidate early invasion events in squids [26,27] and bacterial dynamics in filter feeding oysters [28].

In the present study, we have investigated infection dynamics of *V. splendidus* 10/068 1T1 in *Mytilus edulis*. We describe (i) the development of an experimental infection model by water tank cohabitation with septic mussels, (ii) the localization of GFP bacteria in infected animals with the corresponding tissue lesions and (iii) *in vitro*/*in vivo* interactions between the pathogenic *Vibrio* strain and *Mytilus edulis* hemocytes.

2. Material and methods

2.1. Mussel collection

Adult mussels, *M. edulis* with shell length ranging from 4 to 5 cm, were collected on the intertidal rocky shore of Yport (0°18'52"E:49°44'30"N, France) between December 2015 and March 2016, immediately transported to the laboratory and placed in a temperature-controlled (10°C) aerated Biotop Nano Cube 60 seawater tank (Sera, Heinsberg, Germany) , equipped with mechanical and activated biological filtering. The animals were fed with algae (*Isochrysis galbana*) and maintained in these conditions for at least one week before use.

2.2. Bacterial strains and culture conditions

Two parental and GFP-tagged *V. splendidus*-related strains were used in this study: a virulent *V. splendidus* 10/068 1T1 isolated from mussel mortality events reported by professional (French national surveillance network REPAMO) in 2010 and an innocuous *V. splendidus* 12/056 M24T1 isolated from mussel microflora in absence of mortality in the context of Bivalife European project in 2012 [11]. Bacteria were routinely cultivated overnight in LBS [Luria Bertani complemented with salt, NaCl 20 $g.L^{-1}$ (f.c.)] at 22°C. Stock cultures were stored at -80°C in LBS with glycerol 15% (v/v) supplemented with kanamycin 100 $\mu g.L^{-1}$ for GFP-tagged strains.

2.3. *In vitro* hemocyte challenge

2.3.1. Hemolymph collection

Hemolymph was withdrawn from the posterior adductor muscle sinus, by gentle aspiration with a 1 mL syringe equipped with a 22G needle. Quality of samples was systematically checked by microscopic observation before using in bioassays. Samples containing protozoa, tissue fragments, low number of hemocytes were discarded.

2.3.2. Hemocyte adhesion

Cells were incubated with bacteria at a ratio of 10 bacteria/hemocyte, or with sterile physiological water (NaCl 9 $g.L^{-1}$), in a 24-well tissue-culture plates (Greiner). After 2, 4 and

6 hours at 15°C, the number of non adherent cells in the supernatant was counted by flow cytometer.

2.3.3. Acidic vacuole formation

Crude hemolymph was placed into individual wells of 24-well tissue-culture plates (Greiner) for cytometry or in 35 mm µ-Dish (Ibidi) for microscopy. Cells were exposed to *Vibrio* strains at 10:1 ratio (bacteria:hemocytes) for 2 hours at 15°C.

Lysotracker (LysoTracker® Green DND-26, life technologies) at 2 µM was added and cells were incubated for 30 minutes at 15°C in the dark. Hemocyte fluorescence was quantified by flow cytometry. For microscopy imaging, cells were washed with the marine physiological saline solution [MPSS (470 mM NaCl, 10 mM KCl, 10 mM $CaCl_2$, 10 mM HEPES, 48,7 mM $MgSO_4$), pH 7.8, 0.2 µm filtered]. Hemocyte nuclei were counterstained with hoechst 33342 (5 µM, 15 min) and imaged by epifluorescence microscopy.

2.3.4. Hemocyte viability

Hemocytes were exposed to bacteria (10/068 1T1 and 12/056 M24T1) at 10^8 CFU.mL^{-1} for different time periods (2, 4, 6, 18 and 24h) at 15°C. At each time point, propidium iodide was added (20 µM) and cell viability was measured by flow cytometry.

2.4. *In vivo* challenge

2.4.1. Mussel infection by water tank cohabitation model

Bacteria were prepared at OD_{600nm} of 1 as described in Ben Cheikh et al. [11]. Animals were anesthetized for 2–3 h at 16°C in a magnesium chloride solution (50 g.L^{-1}, 1/4: v/v seawater/freshwater) under aeration. Subsequently, a volume of 100 µL of bacterial suspension (2.10^8 CFU.mL^{-1}) or filtered sterile seawater (FSSW) for the negative control was injected into the posterior adductor muscle. After injection, the animals were transferred to tanks (3 replicate tanks, 10 mussels per tank) filled with 2L of UV-treated and filtered seawater supplemented with 50 mL of phytoplankton (*Isochrysis galbana*). After 24 hours, moribund animals were sacrificed by severing their adductor muscle and placed in cohabitation with a group of 10 apparently healthy mussels. For the negative control, mussels injected with FSSW (alive) were sacrificed and used in the same conditions. After 72 hours of cohabitation, injected mussels were removed. During the experiment, animals were maintained under static conditions at 16°C with aeration. Mortality was monitored each day over a six days period. Animals were considered to be dead when the valves did not close following stimulation. Newly dead mussels were removed from the tanks.

2.4.2. Bacteria counting in seawater

Seawater was sampled from cohabitation tanks each day during the experiment period. 100 µL of samples serially diluted in sterile physiological water (NaCl 9 $g.L^{-1}$) was plated on LBS agar supplemented with kanamycin 100 $\mu g.L^{-1}$. After 48h at 22°C, colonies were counted. The presence of GFP colonies was verified under a fluorescence stereo microscope (Leica microsystems).

2.4.3. Hemocyte cellular parameters analysis

Hemolymph was sampled from exposed mussels and mixed with cold Alsever's solution (300 mM NaCl, 100 mM Glucose, 30 mM sodium Citrate, 26 mM citric acid, 10 mM EDTA, pH 5.4) for cytometry analysis.

Variation in hemocyte count and the percentage of cells containing GFP-tagged bacteria was determined. Cell viability was investigated by adding propidium iodide (20 µM).

2.4.4. Histological and Immunohistochemical analyses

During cohabitation infection, mussels were sampled at different time periods and removed from their shell. Tissues were fixed in Davidson's solution (20% formaldehyde 36%, 30% FSSW, 10% glycerol, 30% ethanol 95% and 10% acetic acid) for 48h, dehydrated in a graded series of ethanol, and embedded in paraffin. Consecutive 3-5 µm thick sections were adhered to Superfrost [hematoxylin-eosin (HE) staining] or Superfrost Plus [immunohistochemistry (IHC)] microscope slides.

For tissue examination, sections were stained by classical hematoxylin-eosin protocol. Presence of listed pathogens (*Bonamia* sp., *Marteilia* sp., *Perkinsus* sp. and *Mikrocytos* sp.) was examined as well as trematods, copepods, *Mytilicola*, ciliates and gregarines. For lesions, we noticed the presence of necrosis, bacterial "foyer", hemocytes infiltration and granulomas into the different tissues: gills, gonads, digestive glands, mantle, muscle, kidney and digestive tube. The lesions in each organ were coded as follows: 0 (absence of lesion); 1 (low), 2 (moderate), 3 (high). "Low" corresponds to at least one observation in 20 fields of the slide, "moderate" corresponds to at least 5 observations in 10 fields of the slide and "high" corresponds to at least 10 observations in 10 fields of the slide.

For IHC, a polyclonal antibody raised in rabbit against recombinant full length GFP protein was used (Ab290, Abcam). The specificity of this antiserum has been previously tested and optimized. Immuno-labellings were performed with a Benchmark automate (Ventana-Roche) by Histalim (Montpellier). Sections were incubated for 32 min with primary antibody (1:5000) and revealed with Ultraview Red Alkaline Phosphatase kit (Roche Diagnostics). Slides were

finally numerized with a Nanozoomer x20 (Hamamatsu). Labeling of bacterial-like cells was coded following the same criteria used for lesion observations: 0 (absence of labelling); 1 (low), 2 (moderate), 3 (high).

2.5. Statistical analyses

Statistical analysis was performed by using SigmaPlot 12 (Systat Software Inc., Chicago, IL). Replicates were averaged and the values were tested for normality (Shapiro-Wilk) and paired comparisons were performed by Student's t-tests or by Mann-Whitney rank sum tests in case of unequal variance. Statistical significance was accepted for *$p < 0.05$, **$p < 0.01$ or ***$p < 0.001$.

3. Results

3.1. Hemocyte adhesion

The effect of *V. splendidus*-related strains on hemocyte-substrate adhesion was evaluated *in vitro* for different time of incubation (**Figure 1**). Hemocyte attachment to the culture dish was significantly affected after 2h of exposure to the virulent *V. splendidus* 10/068 1T1. Moreover, the number of detached hemocytes increased for 6h incubations. In contrast, when exposed to the innocuous *Vibrio* strain 12/056 M24T1, non-adherent cells increased slightly after 2h exposure and then decreased.

3.2. Acidic vacuole formation

The capacity of *M. edulis* hemocytes to generate phagolysosome proliferation after exposure to virulent and non-virulent bacteria in *vitro* was investigated by flow cytometry and epifluorescence microscopy (**Figure 2**). The lysotracker signal, indicative of acidic vacuole formation, was significantly higher in hemocytes challenged with the strain 12/056 M24T1 than in cells co-cultured with the strain 10/068 1T1 ($p<0.001$, **Figure 2a**). Moreover, in the case of exposure to 12/056 M24T1, numerous phagolysosomic compartments surrounding the nucleus can be found (**Figure 2b**). Microscopic observation also confirmed the absence of large acidic compartments in cells challenged with the virulent strain.

3.3. Hemocyte viability

Hemocyte viability was monitored after exposure to *V. splendidus*- related strains for different time durations. Cell viability was stable during the first 6 hours for both strains with values corresponding to 92% of viable cells (**Figure 3**). Then, hemocyte viability slightly decreased until 24h post exposure to the innocuous strain 12/056 M24T1, but was never lower than 80 %.

In contrast, for the same time periods, the viability of cells incubated with the strain 10/068 1T1 was significantly affected, reaching a percentage of viable cells of only 59% after 24h exposure to the virulent strain.

3.4. *Vibrio* infection by cohabitation challenge

Experimental infection of mussels with the pathogenic *V. splendidus* 10/068 1T1 was obtained by water tank cohabitation assays. First mortalities appeared after 3 days (16.6%) and increased progressively to reach almost 45% at the 6^{th} day (**Figure 4**). No mortality was observed in control tanks.

3.5. Seawater bacteria count during infection

Bacteria seawater density in cohabitation tanks was monitored during infection (**Figure 5**). After 48h of cohabitation, the *Vibrio* density reached 3.10^6 CFU/mL, then decreased progressively to 2.10^3 CFU/mL after 5 days.

3.6. Hemocyte parameters analysis during the experimental infection

Different hemocyte parameters were investigated during cohabitation assays with septic mussels infected by the virulent strain 10/068 1T1 (**Figure 6**). In hemolymph sampled from the adductor muscle, the total hemocyte count increased significantly 48h after the cohabitation onset and then decreased until the end of the exposure to reach control values (**Figure 6a)**. Interestingly, GFP bacteria were detected in hemocytes. The percentage of cells containing GFP-tagged *Vibrio* was also higher at the beginning of the exposure and then decreased progressively (**Figure 6b**). Furthermore, hemocyte viability slightly decreased compared to the control but remained almost stable during *Vibrio* infection (80% of viable cells at day 2 and 74% at day 5, **Figure 6c**).

3.7. Tissue infection by bacteria

GFP-*Vibrios* were detected mainly in gills of 8 out of 31 live animals and 9 out of 9 moribund animals, either in the pallial cavity, forming aggregates, attached to apical cilia or between ordinary gill filaments (**Figure 7A, C**). Some labeling were also noticed in esophagi or stomach of 4 out of 28 live animals (**Figure 7D**). Main observed lesions correspond to necrosis of epithelia (gills and digestive tissues, respectively 30 and 8 out of 40 animals) and hemocyte infiltrations (17 out of 40 animals), as well as granulomas in the mantle (17 out of 40 animals) (**Figure 7B, supplementary figure 1C-E, Table 1**). Moribund animals contained bacteria in large amounts and presented general necrosis patterns even if some organs were obviously not affected (muscle, gonad, kidney and mantle) (**Figure 7B, Table 1**).

Some trematodes *metacerca* in 36 out of 40 animals, copepods in 3 out 40 animals, ciliates in 28 out of 40 animals or gregarines in 7 out of 40 animals, were noticed (**supplementary figure 1**, **Table 1**). However, the most noticeable microorganism present on hematoxylin-eosin strained slides corresponds to bacteria. Seventeen of the 40 analyzed individuals present bacterial cells into gills (8 low amount, 6 moderate and 3 high). Bacteria were also noticed in digestive tissues (10 individuals – 6 low and 4 moderate) and mantle (9 individuals – 3 low and 6 moderate) (**supplementary figure 1D, Table 1**). No listed parasites were found in the 40 mussels (19 females and 21 males).

4. Discussion

In a previous study, we have reported the virulence of *V. splendidus* 10/068 1T1 to the blue mussel and its capacity to alter the host immune response [11]. Herein, we expand the knowledge on mussel-pathogen interactions by exploring infection dynamics via water tank cohabitation experimental model and by studying hemocyte responses via *in vitro/in vivo* assays.

4.1. *In vitro* hemocyte-pathogen interactions

To elicit cell-mediated immune responses, adhesion phenomena are crucial. In our experiments, *V. splendidus* 10/068 1T1 severely altered hemocyte attachment to the culture substratum. After 2 hours of incubation in the presence of the virulent *Vibrio*, the number of non-adherent cells was higher than in non-treated cultures or in cells co-incubated with the innocuous bacteria. This effect increased after 6h of exposure to *V. splendidus* 10/068 1T1. Similar observations were made for other *Vibrio* species with bivalve hemocytes. For example, *V. tasmaniensis* LGP32 decreased hemocyte adhesion capacity in *Mytilus edulis* [29], *Mytilus galloprovincialis* [30] and *Mya arenaria* [31]. The same response was reported for *Crassostrea gigas* hemocytes challenged with *V. aestuarianus* 01/32 [32] and cells of *Ruditapes philippinarum* in contact with *V. tapetis* [33]. Despite the robustness of these observations, specific mechanisms by which a pathogen induces hemocyte detachment from adhesion surfaces remain poorly understood. Some studies suggested the involvement of proteases secreted by the bacteria and responsible for disruption of cytoskeleton, cell adhesion molecules and extracellular matrix components. In the Pacific oyster, hemocyte treatment with extracellular products (ECPs) of *V. aestuarianus* 01/32 or *V. tubiashii* 07/118 T2 inhibited cell binding to culture dish [34,35]. Furthermore, the hydrolytic action of extracellular effectors capable to degrade muscle collagen, bovine actin and fibronectin proteins has been shown [35]. In addition of abolishing hemocyte attachment to substrate, alteration of immunocyte adhesion capabilities by ECPs also

probably affects phagocyte activity. In this regard, we have previously shown that ECPs from *V. splendidus* 10/068 1T1 inhibit *M. edulis* hemocyte phagocytosis [11].

Upon entrance into hemocytes, the fate of bacteria depends on phagosome biogenesis and maturation. Intracellular trafficking and killing of engulfed microorganisms is a highly choreographed process driven by subsequent fusion and fission events during which the maturing phagosome acquires the characteristics of degradative acidic lysosomes [36,37]. In our study, *V. splendidus* 10/068 1T1 inhibited acidic vacuole formation in mussel hemocytes while the innocuous phylogenetically related to *V. splendidus* 12/056 M24T1 had no effect. Such mechanism has been described for intracellular pathogens as strategy to survive and maintain infection within cells. This is the case of *Legionella pneumophila*, the causative agent of Legionnaire's pneumonia, known for its ability to manipulate host cell vesicular trafficking pathways and to inhibit phagosome-lysosome fusion [38,39]. In the same way, *Mycobacterium* sp. reside inside vacuoles and arrest the fusion with late endosomal/lysosomal organelles [40, 41]. For *Vibrio* species, few reports have shown their capacity to adopt intracellular stages [42–44]. To our knowledge, only *V. tasmaniensis* LGP32 has been described as a facultative intracellular pathogen of the Pacific oyster, able to modulate phagosome maturation as well as oxidative response [24]. More recently, Vanhove et al. [45] showed the intracellular surviving of this strain until hemocyte cytolysis (more than 25% of cell lysis after 17h incubation). In accordance with these findings, it seems that *V. splendidus* 10/068 1T1 displays a similar infection strategy to *V. tasmaniensis* LGP32. Besides altering phagosome maturation and ROS production [11], this *Mytilus edulis* pathogen affected hemocyte viability and induced almost 39% of dead cells after 18h. The latter point prove the cytotoxicity of the bacteria and suggests its surviving into the cells.

4.2. *In vivo* infection dynamics

Understanding pathogenesis processes requires an animal model of infection [46]. In our previous study, we have demonstrated the virulence of *V. splendidus* 10/068 1T1 towards the blue mussel by injection [11]. In spite its efficacy and repeatability, this method does not reflect the realistic way of host-bacteria interaction. Herein, we successfully reproduced experimental infection by cohabitation assays. In these experimental conditions, first mortalities appeared after 3 days and increased progressively suggesting a necessity of time for bacteria transfer from diseased animals and the occurrence of a latency period in healthy mussels. At the same time intervals, the amount of GFP-*Vibrio* released in the seawater decreased (3.10^6 CFU/mL at the 2nd day to 2.10^3 CFU/mL at the 6th day). In addition to probable adhesion/penetration into

its host, this decline could result from bacteria mortality or adhesion to tank walls. Though, *Vibrio* were also detected in healthy mussel tissues confirming a transmission of a part of them from infected animals during the cohabitation period.

Up to now, only few works have investigated non-invasive methods for the study of infectious diseases in bivalves and they were limited to Pacific oysters. In this model, successful experimental vibriosis were induced by cohabitation [47,48] or by immersion assays [49]. In our case, unlike cohabitation experiments, the bathing procedure did not cause any mortality (data not shown). This negative result reveals the complexity of infection process. Bacteria may require a priming infectious niche or a cooperation with mussel microflora to initiate some virulence mechanisms [50].

During experimental infection, the number of circulating cells temporary increased at day 2 post-challenge and then stabilized to a value not distinct from control. Similar transient hemocytosis have been described in diverse bivalve species like *M. edulis* [51], *M. galloprovincialis* [52] and *R. philippinarum* [53] in response to physical stresses or pathogen threats. Such variation in circulating hemocytes have been explained by cell proliferation [51]. Mobilizations of peripheral hemocytes from tissues consecutively to bacterial infection were also evoked to account for by a transient increase of circulating cells [32,53]. Inversely, back infiltration of infected sites by hemocytes could explain a consecutive decrease of total hemocyte count in hemolymph. Alternatively, the decrease of cell concentration observed secondarily to hemocytosis can also originate from a *Vibrio* induced hemocyte death. The hypothesis get confirmation from our experiments showing a loss of viability both for hemocytes exposed to *Vibrio in vitro* and for hemocytes withdraw from infected animals. It is also in good agreement with mortalities observed after 3 days of cohabitation with septic mussels. Furthermore, *V. splendidus* 10/068 1T1 was detected in hemocytes and the population of bacteria-containing hemocyte declined progressively with time. The latter result is probably coherent with a pathogenicity involving a phagocyte lysis and a bacteria release.

In addition to hemocyte parameters analysis, histology was performed on infected mussels. Many organisms were identified in tissues of living and moribund mussel (trematodes, copepods, *Ciliophora*, ciliates and gregarines). The presence of parasites is not surprising since animals were collected from natural areas. Their potential interaction with pathogens are still unknown. GFP-*Vibrio* were localized in diverse organs and obviously caused necrosis of digestive gland and gills principally. Data concerning bacterial diseases in bivalves indicate that infections are initiated at mucosal interfaces [54]. Nevertheless, in order to establish a

chronology, the entry route of bacteria has to be identified. Few studies explored portal access of pathogens in bivalves. For example, the organic matrix of the shell has been described as a putative entryway of the pathogenic *V. tapetis* in the clam *R. philippinarum* [55,56]. More recently, a study suggested the involvement of hemocytes in microbe transport because of their ability to migrate across mucosal epithelia and to translocate within hours from pallial surfaces to underlying tissues and to the circulatory system [54]. This hypothesis may be plausible in our study considering the cytotoxicity of *V. splendidus* 10/068 1T1 to hemocytes. Further investigations at the first hours of infection are needed to elucidate whether hemocytes are the first or the last target of pathogens.

5. Conclusion

V. splendidus 10/068 1T1 has been previously reported to be pathogenic to the blue mussel. In this study, we first investigated hemocyte-bacteria interactions. *In vitro* challenges demonstrate the capacity of *Vibrio* strain to alter the maturation of the phagolysosome, the cell adhesion and viability. Then, we successfully established a non-invasive experimental infection model via cohabitation. Bacteria were able to bypass defense barriers and were detected in diverse organs and in hemocytes. The number and the viability of circulating hemocytes were altered. Taken together, our results confirm the virulence of *V. splendidus* 10/068 1T1 towards *M. edulis* hemocytes and suggest the use of immune cells as pathogen vehicles to spread the infection in the whole organism. Furthermore, besides the description of an original infection process, this study can be useful to be compared with natural mortalities occurred in the field.

Acknowledgements

This work received fundings from the State/Region Plan Contract (CPER) allocated through the Research Federation FR CNRS 3730 SCALE /FED 4116 SCALE (Sciences Appliquées à L'Environnement), and DGAl support through National Reference Laboratory activities for mollusc diseases (Ifremer-La Tremblade). Yosra Ben Cheikh was a recipient for a Ph.D. grant from the Conseil Regional de Haute-Normandie. The authors are indebted to the marine fish farm Aquacaux (Octeville, France) and Histalim (Montpellier, France) for valuable technical assistance.

References

379 [1] Thompson, F.L., Iida, T., Swings, J., **2004**. Biodiversity of *Vibrios*. *Microbiol. Mol. Biol.*
380 *Rev*. 68, 403–431. doi:10.1128/MMBR.68.3.403-431.2004
381 [2] Hasan, N.A., Grim, C.J., Lipp, E.K., Rivera, I.N.G., Chun, J., Haley, B.J., Taviani, E.,
382 Choi, S.Y., Hoq, M., Munk, A.C., Brettin, T.S., Bruce, D., Challacombe, J.F., Detter,
383 J.C., Han, C.S., Eisen, J.A., Huq, A., Colwell, R.R., **2015**. Deep-sea hydrothermal vent
384 bacteria related to human pathogenic *Vibrio* species. *Proc. Natl. Acad. Sci*. 112, E2813–
385 E2819. doi:10.1073/pnas.1503928112
386 [3] Travers, M.-A., Boettcher Miller, K., Roque, A., Friedman, C.S., **2015**. Bacterial
387 diseases in marine bivalves. *J. Invertebr. Pathol*. doi:10.1016/j.jip.2015.07.010
388 [4] Feldhusen, F., **2000**. The role of seafood in bacterial foodborne diseases. *Microbes*
389 *Infect.* 2, 1651–1660. doi:10.1016/S1286-4579(00)01321-6
390 [5] Powell, J.L., **1999**. *Vibrio* species. *Clin. Lab. Med.* 19, 537–552, vi.
391 [6] Colwell, R.R., Grimes, D.J., **1984**. *Vibrio* diseases of marine fish populations.
392 *Helgoländer Meeresunters*. 37, 265–287. doi:10.1007/BF01989311
393 [7] Ben-Haim, Y., Rosenberg, E., **2002**. A novel *Vibrio* sp. pathogen of the coral
394 *Pocillopora damicornis*. *Mar. Biol*. 141, 47–55. doi:10.1007/s00227-002-0797-6
395 [8] Goarant, C., Ansquer, D., Herlin, J., Domalain, D., Imbert, F., De Decker, S., **2006**.
396 "Summer Syndrome" in *Litopenaeus stylirostris* in New Caledonia: Pathology and
397 epidemiology of the etiological agent, *Vibrio nigripulchritudo*. *Aquaculture* 253, 105–
398 113. doi:10.1016/j.aquaculture.2005.07.031
399 [9] Paillard, C., Le Roux, F., Borrego, J.J., **2004**. Bacterial disease in marine bivalves, a
400 review of recent studies: Trends and evolution. *Aquat. Living Resour*. 17, 477–498.
401 doi:10.1051/alr:2004054
402 [10] Beaz-Hidalgo, R., Balboa, S., Romalde, J.L., Figueras, M.J., **2010a**. Diversity and
403 pathogenecity of *Vibrio* species in cultured bivalve molluscs. *Environ. Microbiol. Rep*.
404 2, 34–43. doi:10.1111/j.1758-2229.2010.00135.x
405 [11] Ben Cheikh, Y., Travers, M.-A., Morga, B., Godfrin, Y., Rioult, D., Le Foll, F., **2016**.
406 First evidence for a *Vibrio* strain pathogenic to *Mytilus edulis* altering hemocyte immune
407 capacities. *Dev. Comp. Immunol.* 57, 107–119. doi:10.1016/j.dci.2015.12.014
408 [12] Kwan, T.N., Bolch, C.J.S., **2015**. Genetic diversity of culturable *Vibrio* in an Australian
409 blue mussel *Mytilus galloprovincialis* hatchery. *Dis. Aquat. Organ*. 116, 37–46.
410 doi:10.3354/dao02905
411 [13] Bruto, M., James, A., Petton, B., Labreuche, Y., Chenivesse, S., Alunno-Bruscia, M.,
412 Polz, M.F., Le Roux, F., **2017**. *Vibrio crassostreae*, a benign oyster colonizer turned into
413 a pathogen after plasmid acquisition. *ISME J.* 11, 1043–1052.
414 doi:10.1038/ismej.2016.162
415 [14] Gay, M., Berthe, F.C.J., Le Roux, F., **2004**. Screening of *Vibrio* isolates to develop an
416 experimental infection model in the Pacific oyster *Crassostrea gigas*. *Dis. Aquat. Organ*.
417 59, 49–56. doi:10.3354/dao059049
418 [15] Lacoste, A., Jalabert, F., Malham, S., Cueff, A., Gélébart, F., Cordevant, C., Lange, M.,
419 Poulet, S.A., **2001**. A *Vibrio splendidus* strain is associated with summer mortality of
420 juvenile oysters *Crassostrea gigas* in the Bay of Morlaix (North Brittany, France). *Dis.*
421 *Aquat. Organ*. 46, 139–145. doi:10.3354/dao046139
422 [16] Lemire, A., Goudenège, D., Versigny, T., Petton, B., Calteau, A., Labreuche, Y., Le
423 Roux, F., **2015**. Populations, not clones, are the unit of *Vibrio* pathogenesis in naturally
424 infected oysters. *ISME J.* 9, 1523–1531. doi:10.1038/ismej.2014.233
425 [17] Saulnier, D., De Decker, S., Haffner, P., Cobret, L., Robert, M., Garcia, C., **2010**. A
426 large-scale epidemiological study to identify bacteria pathogenic to Pacific oyster
427 *Crassostrea gigas* and correlation between virulence and metalloprotease-like activity.
428 *Microb. Ecol*. 59, 787–798. doi:10.1007/s00248-009-9620-y

[18] Lambert, C., Nicolas, J.L., Cilia, V., **1999**. *Vibrio splendidus*-related strain isolated from brown deposit in scallop (*Pecten maximus*) cultured in Brittany (France). *Bull Eur Fish Pathol* 102.

[19] Nicolas, J.L., Corre, S., Gauthier, G., Robert, R., Ansquer, D., **1996**. Bacterial problems associated with scallop *Pecten maximus* larval culture. *Dis. Aquat. Org*. 27, 67–76. doi:10.3354/dao027067

[20] Beaz-Hidalgo, R., Diéguez, A.L., Cleenwerck, I., Balboa, S., Doce, A., de Vos, P., Romalde, J.L., **2010b**. *Vibrio celticus* sp. nov., a new *Vibrio* species belonging to the *Splendidus* clade with pathogenic potential for clams. *Syst. Appl. Microbiol*. 33, 311–315. doi:10.1016/j.syapm.2010.06.007

[21] Kesarcodi-Watson, A., Kaspar, H., Lategan, M.J., Gibson, L., **2009**. Two pathogens of Greenshell mussel larvae, *Perna canaliculus*: *Vibrio splendidus* and a *V. coralliilyticus/neptunius*-like isolate. *J. Fish Dis.* 32, 499–507. doi:10.1111/j.1365-2761.2009.01006.x

[22] Araya, M.T., Siah, A., Mateo, D.R., Markham, F., McKenna, P., Johnson, G.R., Berthe, F.C.J., **2009**. Morphological and molecular Effects of *Vibrio splendidus* on hemocytes of softshell clams, *Mya arenaria*. *J. Shellfish Res*. 28, 751–758. doi:10.2983/035.028.0403

[23] Balbi, T., Fabbri, R., Cortese, K., Smerilli, A., Ciacci, C., Grande, C., Vezzulli, L., Pruzzo, C., Canesi, L., **2013**. Interactions between *Mytilus galloprovincialis* hemocytes and the bivalve pathogens *Vibrio aestuarianus* 01/032 and *Vibrio splendidus* LGP32. *Fish Shellfish Immunol*. 35, 1906–1915. doi:10.1016/j.fsi.2013.09.027

[24] Duperthuy, M., Schmitt, P., Garzón, E., Caro, A., Rosa, R.D., Le Roux, F., Lautrédou-Audouy, N., Got, P., Romestand, B., de Lorgeril, J., Kieffer-Jaquinod, S., Bachère, E., Destoumieux-Garzón, D., **2011**. Use of OmpU porins for attachment and invasion of *Crassostrea gigas* immune cells by the oyster pathogen *Vibrio splendidus*. *Proc. Natl. Acad. Sci. U. S. A*. 108, 2993–2998. doi:10.1073/pnas.1015326108

[25] Restif, O., Graham, A.L., **2015**. Within-host dynamics of infection: from ecological insights to evolutionary predictions. *Phil Trans R Soc B* 370, 20140304. doi:10.1098/rstb.2014.0304

[26] Nyholm, S.V., Stabb, E.V., Ruby, E.G., McFall-Ngai, M.J., **2000**. Establishment of an animal–bacterial association: Recruiting symbiotic *Vibrios* from the environment. *Proc. Natl. Acad. Sci.* 97, 10231–10235. doi:10.1073/pnas.97.18.10231

[27] Nyholm, S.V., McFall-Ngai, M.J., **2003**. Dominance of *Vibrio fischeri* in secreted mucus outside the light organ of *Euprymna scolopes*: the first site of symbiont specificity. *Appl. Environ. Microbiol.* 69, 3932–3937.

[28] Cabello, A.E., Espejo, R.T., Romero, J., **2005**. Tracing *Vibrio parahaemolyticus* in oysters (*Tiostrea chilensis*) using a Green Fluorescent Protein tag. *J. Exp. Mar. Biol. Ecol*. 327, 157–166.

[29] Tanguy, M., McKenna, P., Gauthier-Clerc, S., Pellerin, J., Danger, J.-M., Siah, A., **2013**. Functional and molecular responses in *Mytilus edulis* hemocytes exposed to bacteria, *Vibrio splendidus*. *Dev. Comp. Immunol*. 39, 419–429. doi:10.1016/j.dci.2012.10.015

[30] Ciacci, C., Betti, M., Canonico, B., Citterio, B., Roch, P., Canesi, L., **2010**. Specificity of anti-*Vibrio* immune response through p38 MAPK and PKC activation in the hemocytes of the mussel *Mytilus galloprovincialis*. *J. Invertebr. Pathol*. 105, 49–55. doi:10.1016/j.jip.2010.05.010

[31] Mateo, D.R., Siah, A., Araya, M.T., Berthe, F.C.J., Johnson, G.R., Greenwood, S.J., **2009**. Differential *in vivo* response of soft-shell clam hemocytes against two strains of *Vibrio splendidus*: Changes in cell structure, numbers and adherence. *J. Invertebr. Pathol*. 102, 50–56. doi:10.1016/j.jip.2009.06.008

[32] Labreuche, Y., Lambert, C., Soudant, P., Boulo, V., Huvet, A., Nicolas, J.-L., **2006a**. Cellular and molecular hemocyte responses of the Pacific oyster, *Crassostrea gigas*, following bacterial infection with *Vibrio aestuarianus* strain 01/32. *Microbes Infect*. 8, 2715–2724. doi:10.1016/j.micinf.2006.07.020

[33] Choquet, G., Soudant, P., Lambert, C., Nicolas, J.-L., Paillard, C., **2003**. Reduction of adhesion properties of *Ruditapes philippinarum* hemocytes exposed to *Vibrio tapetis*. *Dis. Aquat. Organ*. 57, 109–116. doi:10.3354/dao057109

[34] Labreuche, Y., Soudant, P., Gonçalves, M., Lambert, C., Nicolas, J.-L., **2006b**. Effects of extracellular products from the pathogenic *Vibrio aestuarianus* strain 01/32 on lethality and cellular immune responses of the oyster *Crassostrea gigas*. *Dev. Comp. Immunol*. 30, 367–379. doi:10.1016/j.dci.2005.05.003

[35] Mersni-Achour, R., Imbert-Auvray, N., Huet, V., Ben Cheikh, Y., Faury, N., Doghri, I., Rouatbi, S., Bordenave, S., Travers, M.-A., Saulnier, D., Fruitier-Arnaudin, I., **2014**. First description of French *V. tubiashii* strains pathogenic to mollusk: II. Characterization of properties of the proteolytic fraction of extracellular products. *J. Invertebr. Pathol*. 123, 49–59. doi:10.1016/j.jip.2014.09.006

[36] Russell, D.G., 2001. Phagocytosis, in: ELS. John Wiley & Sons, Ltd.

[37] Weiss, G., Schaible, U.E., **2015**. Macrophage defense mechanisms against intracellular bacteria. *Immunol. Rev*. 264, 182–203. doi:10.1111/imr.12266

[38] Horwitz, M.A., **1983**. The Legionnaires' disease bacterium (*Legionella pneumophila*) inhibits phagosome-lysosome fusion in human monocytes. *J. Exp. Med*. 158, 2108–2126.

[39] Isberg, R.R., O'Connor, T., Heidtman, M., **2009**. The *Legionella pneumophila* replication vacuole: making a cozy niche inside host cells. *Nat. Rev. Microbiol*. 7, 13–24. doi:10.1038/nrmicro1967

[40] Armstrong, J.A., Hart, P.D., **1971**. Response of cultured macrophages to *Mycobacterium tuberculosis*, with observations on fusion of lysosomes with phagosomes. *J. Exp. Med*. 134, 713–740.

[41] Russell, D.G., Mwandumba, H.C., Rhoades, E.E., **2002**. *Mycobacterium* and the coat of many lipids. *J. Cell Biol*. 158, 421–426. doi:10.1083/jcb.200205034

[42] Rosenberg, E., Falkovitz, L., **2004**. The *Vibrio shiloi/Oculina patagonica* model system of coral bleaching. *Annu. Rev. Microbiol*. 58, 143–159. doi:10.1146/annurev.micro.58.030603.123610

[43] Santos, M. de S., Orth, K., **2014**. Intracellular *Vibrio parahaemolyticus* escapes the vacuole and establishes a replicative niche in the cytosol of epithelial cells. *mBio* 5, e01506-14. doi:10.1128/mBio.01506-14

[44] Zhang, L., Krachler, A.M., Broberg, C.A., Li, Y., Mirzael, H., Gilpin, C.J., Orth, K., **2012**. Type III effector VopC mediates invasion for *Vibrio* species. *Cell Rep*. 1, 453–460. doi:10.1016/j.celrep.2012.04.004

[45] Vanhove, A.S., Rubio, T.P., Nguyen, A.N., Lemire, A., Roche, D., Nicod, J., Vergnes, A., Poirier, A.C., Disconzi, E., Bachère, E., Le Roux, F., Jacq, A., Charrière, G.M., Destoumieux-Garzón, D., **2016**. Copper homeostasis at the host *Vibrio* interface: lessons from intracellular *Vibrio* transcriptomics. *Environ. Microbiol*. 18, 875–888. doi:10.1111/1462-2920.13083

[46] Le Roux, F.L., Wegner, K.M., Polz, M.F., **2016**. Oysters and **Vibrios** as a Model for Disease Dynamics in Wild Animals. *Trends Microbiol*. 24, 568–580. doi:10.1016/j.tim.2016.03.006

[47] Azéma, P., Travers, M.-A., De Lorgeril, J., Tourbiez, D., Dégremont, L., **2015**. Can selection for resistance to OsHV-1 infection modify susceptibility to *Vibrio aestuarianus*

infection in *Crassostrea gigas*? First insights from experimental challenges using primary and successive exposures. *Vet. Res*. 46. doi:10.1186/s13567-015-0282-0

[48] De Decker, S., Saulnier, D., **2011**. Vibriosis induced by experimental cohabitation in *Crassostrea gigas*: Evidence of early infection and down-expression of immune-related genes. *Fish Shellfish Immunol*. 30, 691–699. doi:10.1016/j.fsi.2010.12.017

[49] De Decker, S., Normand, J., Saulnier, D., Pernet, F., Castagnet, S., Boudry, P., **2011**. Responses of diploid and triploid Pacific oysters *Crassostrea gigas* to *Vibrio* infection in relation to their reproductive status. *J. Invertebr. Pathol*. 106, 179–191. doi:10.1016/j.jip.2010.09.003

[50] Harrison, F., 2013. Bacterial cooperation in the wild and in the clinic: Are pathogen social behaviours relevant outside the laboratory? Bioessays 35, 108–112. doi:10.1002/bies.201200154

[51] Renwrantz, L., Siegmund, E., Woldmann, M., **2013**. Variations in hemocyte counts in the mussel, *Mytilus edulis*: similar reaction patterns occur in disappearance and return of molluscan hemocytes and vertebrate leukocytes. *Comp. Biochem. Physiol. A. Mol. Integr. Physiol*. 164, 629–637. doi:10.1016/j.cbpa.2013.01.021

[52] Ciacci, C., Citterio, B., Betti, M., Canonico, B., Roch, P., Canesi, L., **2009**. Functional differential immune responses of *Mytilus galloprovincialis* to bacterial challenge. *Comp. Biochem. Physiol. B Biochem. Mol. Biol*. 153, 365–371. doi:10.1016/j.cbpb.2009.04.007

[53] Allam, B., Paillard, C., Auffret, M., Ford, S.E., **2006**. Effects of the pathogenic *Vibrio tapetis* on defence factors of susceptible and non-susceptible bivalve species: II. Cellular and biochemical changes following *in vivo* challenge. *Fish Shellfish Immunol*. 20, 384–397. doi:10.1016/j.fsi.2005.05.013

[54] Allam, B., Pales Espinosa, E., **2016**. Bivalve immunity and response to infections: Are we looking at the right place? *Fish Shellfish Immunol*., Special Issue: ISFSI 2016 53, 4–12. doi:10.1016/j.fsi.2016.03.037

[55] Allam, B., Paillard, C., Ford, S.E., **2002**. Pathogenicity of *Vibrio tapetis*, the etiological agent of brown ring disease in clams. *Dis. Aquat. Organ*. 48, 221–231. doi:10.3354/dao048221

[56] Paillard, C., Maes, P., **1995**. The Brown Ring Disease in the Manila Clam, *Ruditapes philippinarum*. *J. Invertebr. Pathol*. 65, 91–100. doi:10.1006/jipa.1995.1015

568

569 **Figure legend**

570 **Figure 1.** Effect of *V. splendidus*-related strains on hemocyte adhesion *in vitro*.
571 The number of non-adherent cells was evaluated after exposure to the virulent *V. splendidus*
572 10/068 1T1 and to the non-virulent *V. splendidus* 12/056 M24T1 for 2, 4 and 6h. Data are
573 expressed as mean ± SEM (n=5), * indicates values significantly different from control and §
574 marks results that significantly differ from values obtained with the non-virulent bacteria
575 12/056 M24T1 ($p<0.05$, Student's t-test)

576 **Figure 2.** Acidic vacuole formation in hemocytes after exposure to *V. splendidus*-related
577 strains. (a) Flow cytometry analysis of hemocytes exposed *in vitro* to virulent or non-virulent
578 bacteria during 2h and incubated 30 min with lysotracker at 0.4 µM. Data are expressed as mean
579 of fluorescence ± SEM, arbitrary units (A.U.), n=5. *** indicates values significantly different
580 from control (Student's t-test, $p<0.001$). (b) Fluorescence microscopy of hemocytes exposed *in*
581 *vitro* to virulent or non-virulent bacteria during 2h and incubated with lysotracker green (0.4
582 µM, 30 min) and Hoechst 33342 (5 µM, 15 min).

583 **Figure 3.** Effect of exposure to bacteria on hemocyte viability *in vitro*. Hemocytes were
584 incubated with *V. splendidus*-related strains 10/068 1T1 or 12/056 M24T1 for different time
585 durations. Viability was determined by flow cytometry after propidium iodide staining. Data
586 are expressed as mean ± SEM, n=4. ** indicates values significantly different from the control
587 $p<0.01$ Student's t-test).

588 **Figure 4.** Cumulative mortalities recorded after experimental infections of adult mussels by
589 water tank cohabitation with septic mussels. GFP-tagged *V. splendidus* 10/068 1T1 strain was
590 injected intramuscularly to mussels. 24h post injection, moribund animals were sacrificed and
591 placed in cohabitation with healthy mussels for 72h and then removed. Cohabitation assays
592 with mussels injected with FSSW were used as control. Data are mean ± SEM of cumulative
593 mortalities in triplicate tanks.

594 **Figure 5.** *V. splendidus* 10/068 1T1 count in water tank seawater during experimental infections
595 *in vivo* by cohabitation with septic mussels. Seawater was sampled daily during cohabitation
596 assays and plated on LBS kanamycin agar plates. Bacteria concentration was determined over
597 time (CFU/mL, mean ± SEM, n=3)

598 **Figure 6.** Analysis of hemocyte parameters during experimental infections by *V. splendidus*
599 10/068 1T1 via water tank cohabitation with septic mussels. Hemolymph was sampled over
600 time from cohabited mussels and (a) absolute hemocyte concentration, (b) percentage of
601 hemocyte containing GFP bacteria and (c) hemocyte viability were monitored by flow
602 cytometry. Data are expressed as mean ± SEM (n=4-13). Values significantly different from
603 control are indicated (* $p<0.05$, ** $p<0.01$*, ***$p<0.001$, Student's t-test).

604 **Figure 7.** Histological observations of mussel tissues during experimental infections by *V.*
605 *splendidus* 10/068 1T1 via water tank cohabitation with septic mussels. GFP-tagged bacteria
606 were detected by immunohistochemistry (pink labeling). Tissues were counter-stained with
607 hematoxylin. A-C: Gills, D: esophagi and stomach. Scale bars of 50 or 100 µm are indicated.

608 **Supplementary figure 1.** Histological observations of hematoxylin-eosin stained sections of
609 mussel tissues during experimental infections by water tank cohabitation with septic mussels.
610 A. Unidentified trematode in digestive glands (metacerca), B. *Mytilicola* sp. in digestive lumen,
611 C. Unidentified copepod and hemocytes infiltration in gills, D. Bacteria, ciliates and gill
612 necrosis, E. Digestive glands and esophagi necrosis, F. Inflammatory granulomas. Scale bars
613 of 100 µm, 250 µm, 500 µm or 1 mm are indicated.

614

615

616

617

618

619

620 **Table 1**: Histological observations on hematoxylin-eosin stained sections of mussel tissues
621 during experimental infections by water tank cohabitation with septic mussels. Presence of
622 micro-organisms and lesions (as necrosis, infiltrations or granulomas) were noticed and
623 classified in categories (0, 1, 2 or 3) as defined in material and methods section. A total of 40
624 individuals were observed (21 males, 19 females; 38 live sacrificed animals, 9 moribunds).
625 Number of observations is indicated, as well as the number of included moribunds in this
626 count (includ. xM = including x moribunds).

627

628

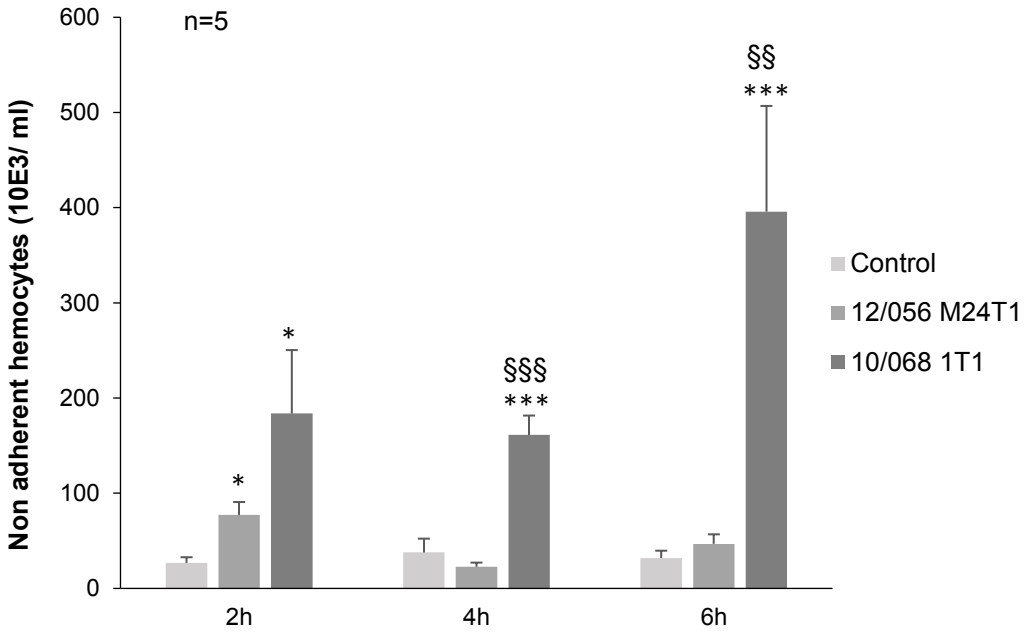
n=5
Non adherent hemocytes (10E3/ ml)
600
500
400
300
200
100
0
2h
4h
6h
*
*
§§§
***
§§
***
Control
12/056 M24T1
10/068 1T1

(a)

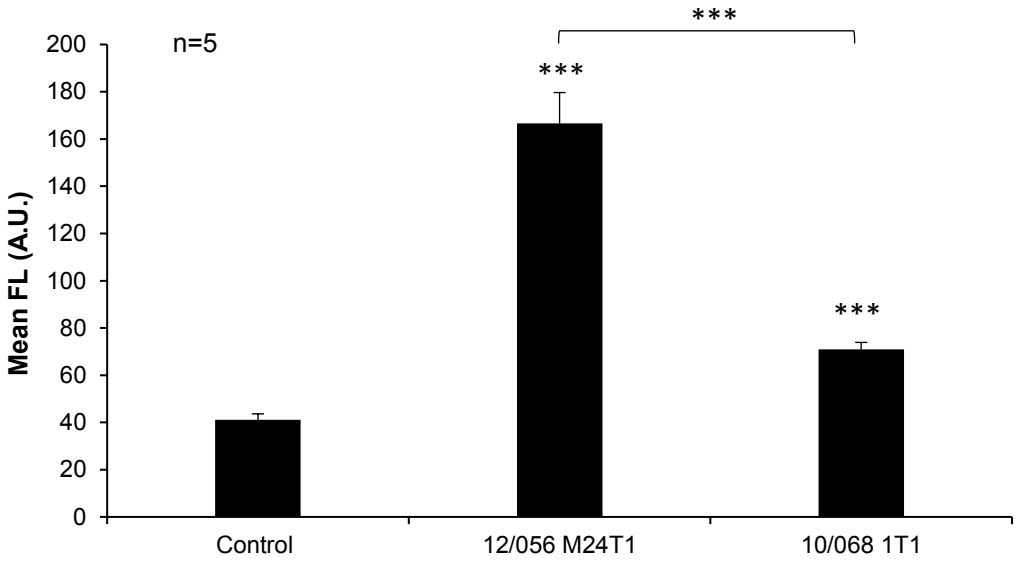
n=5
***
***
***
Mean FL (A.U.)
200
180
160
140
120
100
80
60
40
20
0
Control
12/056 M24T1
10/068 1T1

(b)

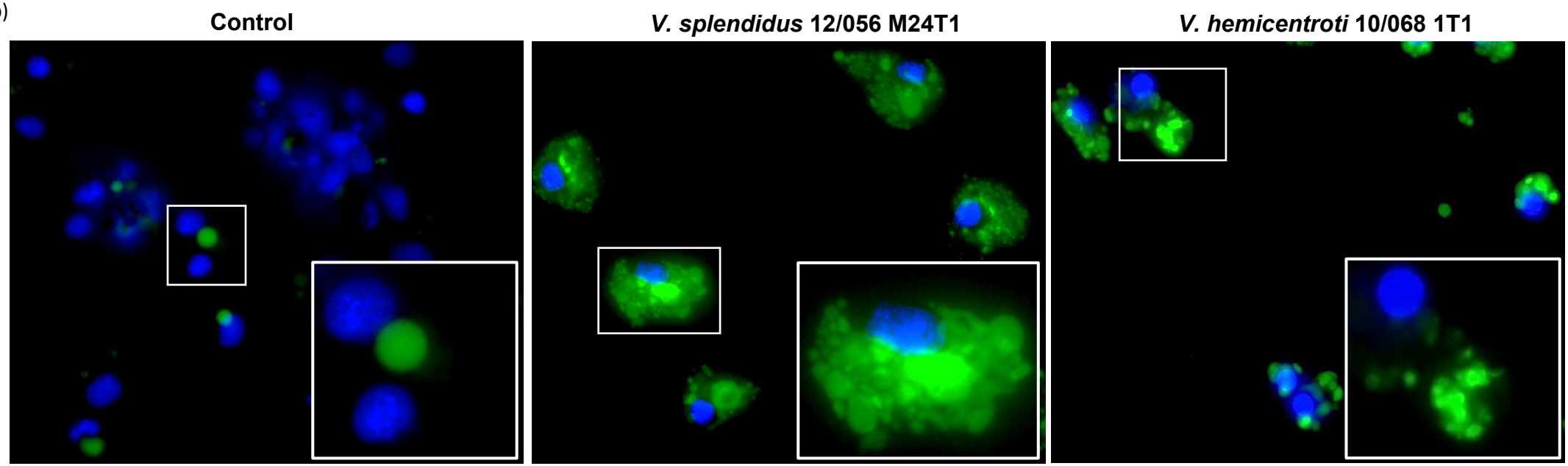
Control
V. splendidus 12/056 M24T1
V. hemicentroti 10/068 1T1

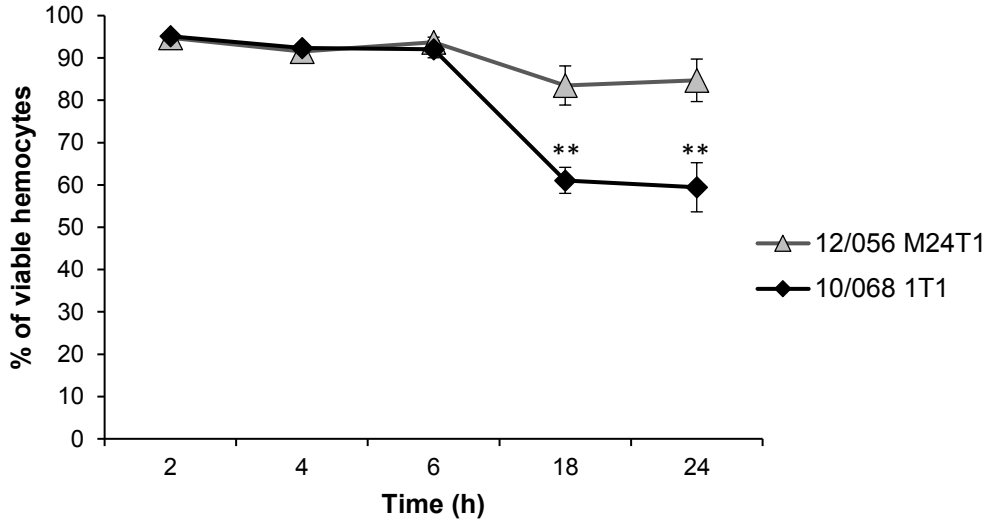
100
90
80
70
60
50
40
30
20
10
0
% of viable hemocytes
2
4
6
18
24
Time (h)
**
**
12/056 M24T1
10/068 1T1

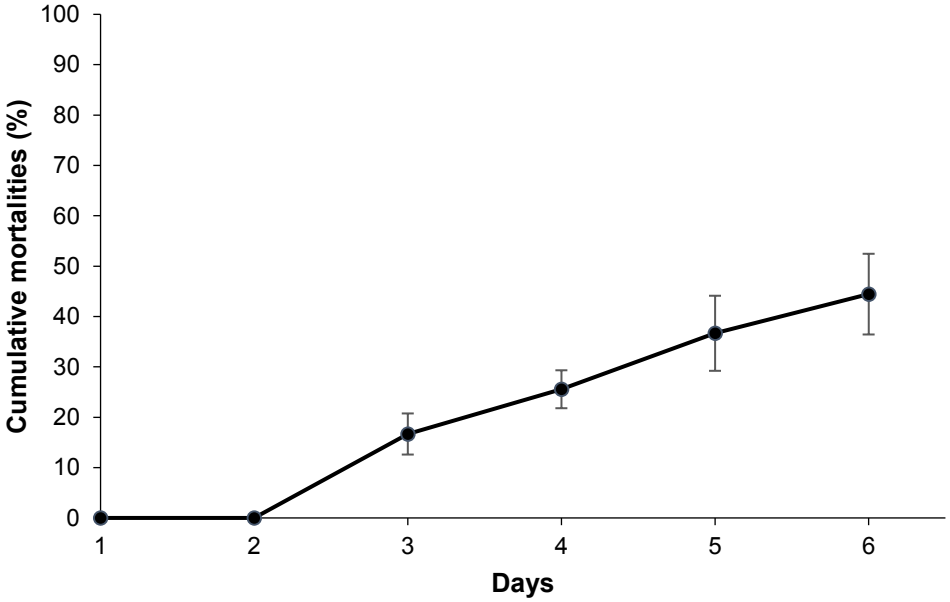
Cumulative mortalities (%)
100
90
80
70
60
50
40
30
20
10
0
1
2
3
4
5
6
Days

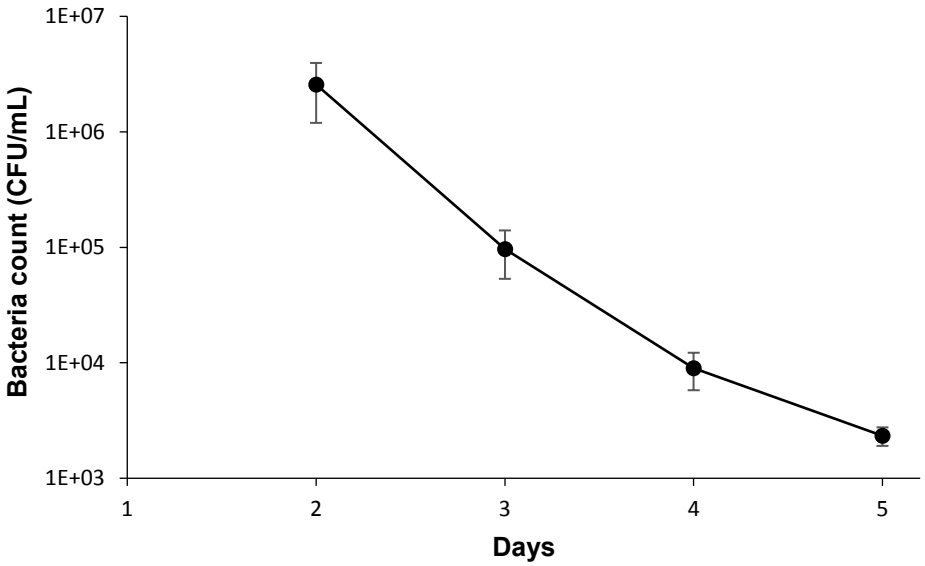
1E+07
1E+06
1E+05
1E+04
1E+03
Bacteria count (CFU/mL)
1
2
3
4
5
Days

(a)

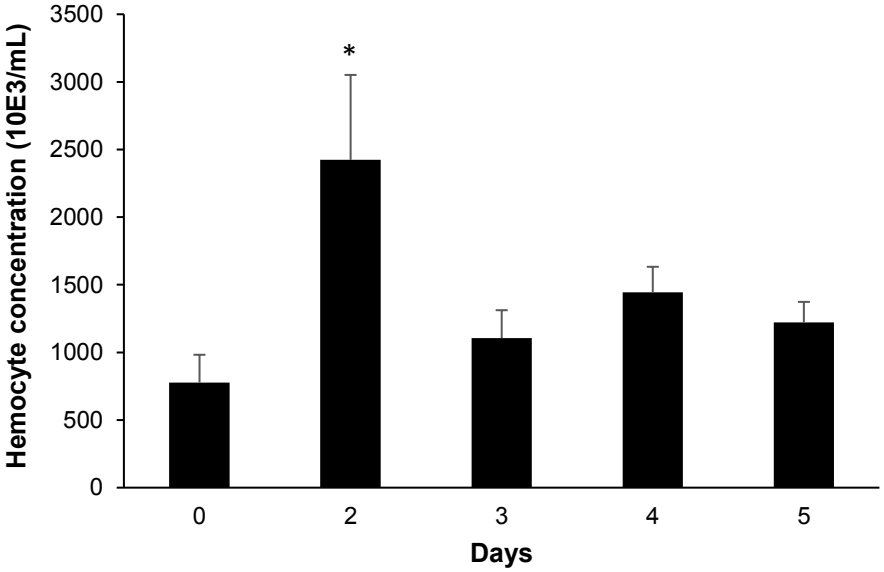
Hemocyte concentration (10E3/mL)
3500
3000
2500
2000
1500
1000
500
0
*
0
2
3
4
5
Days

(b)

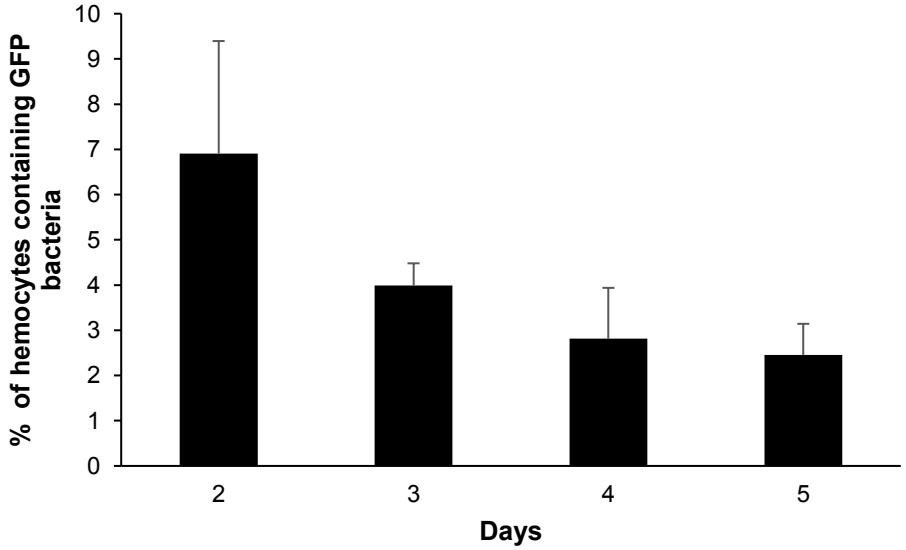
% of hemocytes containing GFP bacteria
10
9
8
7
6
5
4
3
2
1
0
2
3
4
5
Days

(c)

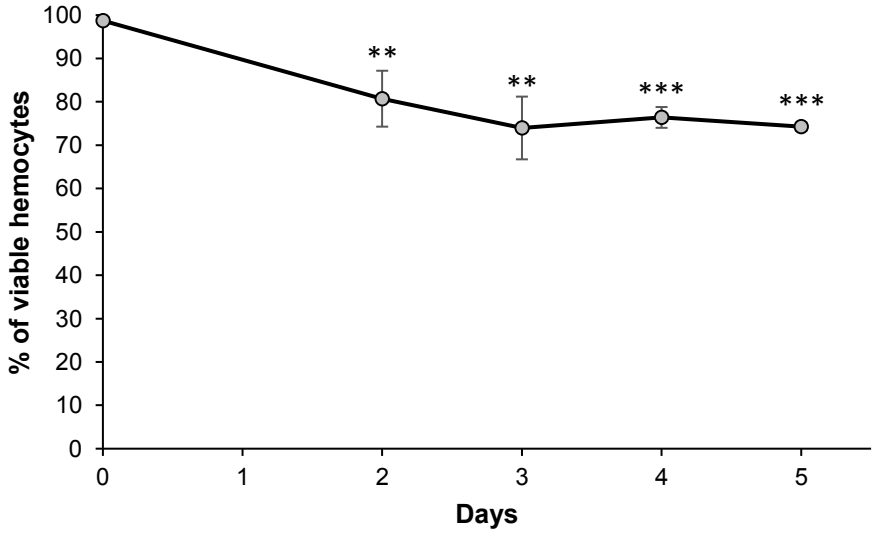
% of viable hemocytes
100
90
80
70
60
50
40
30
20
10
0
**
**
***
***
0
1
2
3
4
5
Days

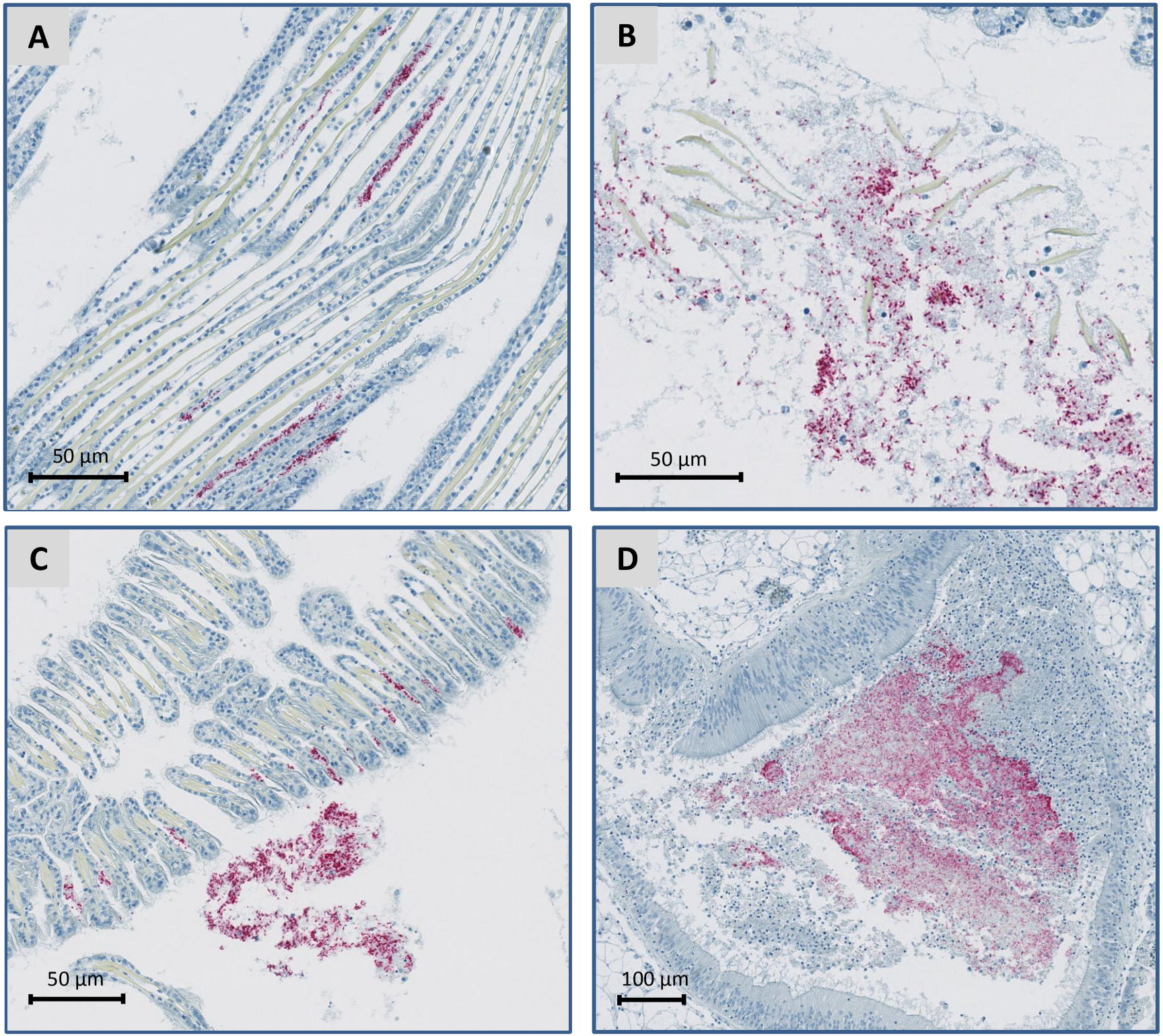
A
50 µm
B
50 µm
C
50 µm
D
100 µm

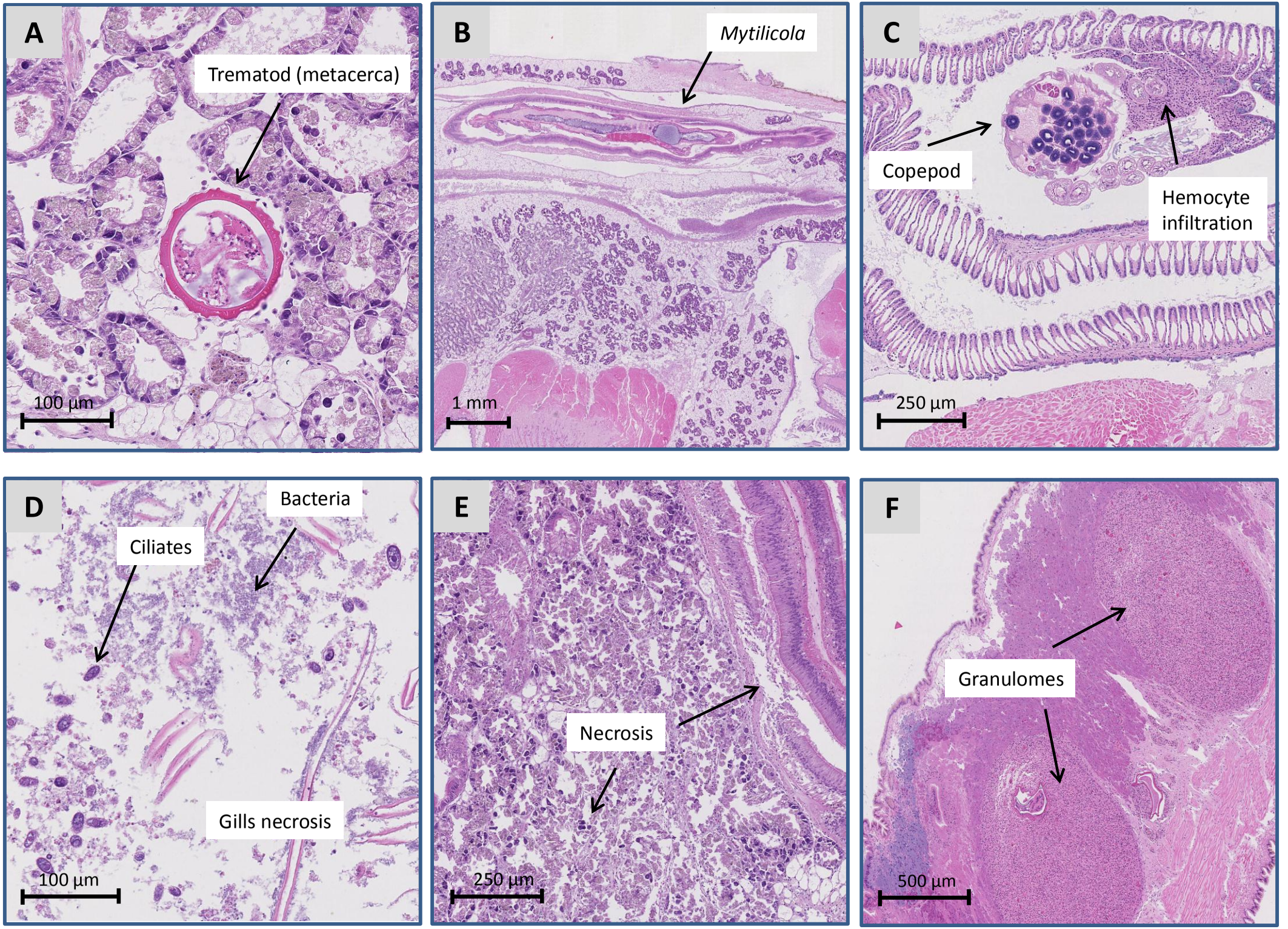
A
Trematod (metacerca)
100 µm
B
Mytilicola
1 mm
C
Copepod
Hemocyte infiltration
250 µm
D
Bacteria
Ciliates
Gills necrosis
100 µm
E
Necrosis
250 µm
F
Granulomes
500 µm

Infection

	Absence (0)	Low (1)	Moderate (2)	High (3)
Presence of noticeable protozoan	40 (includ. 9M)			
Trematods in digestive gland or mantle	4 (includ. 2M)	21 (includ. 5 M)	15 (includ. 2M)	
Copepods (*Mytilicola* sp.) in digestive light	37 (includ. 9M)	3 (includ. 0M)		
Ciliates in digestive gland epithelium	32 (includ. 9M)	1 (include. 0M)	7 (includ. 1M)	
Ciliates in pallial cavity	12 (includ. 1M)	21 (includ. 3M)	5 (includ. 4M)	2 (includ. 1M)
Gregarines in mantle	33 (includ. 7 M)	7 (includ. 2M)		
Bacteria in gills and pallial cavity	23 (includ. 0M)	8 (includ. 4M)	6 (includ. 2M)	3 (includ. 3M)
Bacteria in digestive glands and esophagi	30 (includ. 3M)	6 (includ. 3M)	4 (includ. 3M)	
Bacteria in mantle	31 (includ. 2M)	3 (includ. 1M)	6 (includ. 6M)	
Necrosis of gills	10 (includ. 0M)	20 (includ. 5M)	7 (includ. 1M)	3 (includ. 3M)
Necrosis of digestive gland or esophagi epithelium	32 (includ. 9M)	4 (includ. 1M)	4 (includ. 0M)	
Hemocyte infiltrations in digestive gland, mantle or gills	16 (includ. 4M)	12 (includ. 1M)	12 (includ. 4M)	
Granulomas	23 (includ. 9M)	10 (includ. 0M)	5 (includ. 0M)	2 (includ. 0M)